# ULTRASONIC TECHNIQUES TO CHARACTERIZE PULTRUDED COMPOSITE MEMBERS

By Jerrol W. Littles Jr.,[1] Laurence J. Jacobs,[2] and Abdul-Hamid Zureick[3]

**ABSTRACT:** This paper presents ultrasonic methodologies to measure the engineering constants of pultruded fiber-reinforced polymeric (FRP) composite structural members. These ultrasonic methods have several advantages over mechanical tests, particularly the ability to make a localized measurement of all of the engineering constants in a structural component. This research blends immersion and contact ultrasonic methodologies with surface acoustic wave measurements to completely characterize the elastic properties of FRP specimens. The elastic constants that are measured nondestructively are compared to values measured with mechanical tests (for exactly the same specimens), and the advantages of the ultrasonic methodologies are clearly shown.

## INTRODUCTION

Recent interest in the use of pultruded fiber-reinforced polymeric (FRP) composite members for civil engineering applications has created the need for reliable methods that can completely characterize the engineering constants of these materials. Pultrusion is a manufacturing process consisting of pulling continuous fibers and mats, together with uncured resin, through a dye of constant cross-sectional area. In the dye, the mixture is heated and the resin is cured. Due to the versatility of the manufacturing process, practically any constant cross-sectional member can be made using this process.

Several disadvantages exist in using mechanical methods, such as compression, tension or shear tests, for determining the engineering constants of FRP components. Among these disadvantages are the following:

- The testing procedure itself dictates a specific specimen geometry, and it is therefore impossible to mechanically measure (and compare) all of the engineering constants for a single specimen.
- The dimensions of some shapes can be too small to be mechanically tested in a certain direction [for example, it is impossible to test a 50.8 mm by 50.8 mm (2 in. by 2 in) angle section in the transverse direction].
- Mechanical tests are global in nature, and they cannot provide localized information pertaining to the spatial variations of material properties.
- Constraints of the test procedure (such as the need for a universal testing machine) make them difficult to use in the real-time monitoring of in-service structures.

These limitations of mechanical tests highlight the need for more robust methods to determine the engineering constants of pultruded composite members; this paper examines the viability of one such methodology—ultrasonic testing.

This work uses ultrasonic methodologies to measure the engineering constants of pultruded specimens. These ultrasonic methods have several advantages over mechanical tests.

- All of the engineering constants are measured for a single specimen.
- The measurements are made over a local volume of material, so that it is possible to evaluate spatial variations within a specimen.
- The method examines small specimens (for example, the transverse properties of a 101.6 mm by 101.6 mm angle).
- Ultrasonic techniques do not destroy the specimen, and the potential for in-service monitoring of components or tracking time-dependent material properties exist in long-term tests.

It is important to note that in a mechanical test, a strain gauge measures strain values over a small area of the specimen (~80 $mm^2$). However, the strain experienced by this small area is influenced by the surrounding material (since the entire specimen is being loaded), resulting in more of an average value. In contrast, ultrasonic wave speeds are only influenced by the material through which the wave passes; these ultrasonic techniques provide for a true local measurement of material properties.

This research blends immersion and contact ultrasonic methodologies with surface acoustic wave measurements to completely characterize the elastic properties of pultruded FRP composite structural members. In this study, the surface acoustic waves are generated and detected optically with a Q-switched, pulse laser and a heterodyne interferometer, respectively, whereas the immersion and contact techniques use piezoelectric transducers to generate and detect the ultrasonic waves. The elastic constants that are measured nondestructively are compared to values measured with mechanical tests (for exactly the same specimens), and the advantages of the ultrasonic methodologies are clearly shown.

Previous researchers have used several forms of ultrasonic immersion techniques to measure the elastic constants of various types of composite materials (Zimmer and Cost 1970; Kline and Chen 1988; Stijnman 1995). The application of surface acoustic waves for the characterization of anisotropic materials has been explored using several experimental approaches (Rose et al. 1990; Park and Calder 1994). Kim et al. (1995) used contact transducers and group velocity data to calculate all of the constants of an orthotopic plate. Kim et al.'s dependence on contact transducers makes it difficult to apply this technique to scan large structural components. In contrast, the present study develops a procedure for measuring the entire stiffness matrix (each of the elastic constants) without the restriction of the specimen being placed in an immersion tank. This added flexibility has great advantages over the immersion technique in that a much wider range of specimen sizes and geometries can be evaluated. Surface acoustic wave techniques have great potential for components where immersion is impractical; this research is a vital step toward devel-

[1]Mat. and Mech. Engrg., United Technologies Pratt and Whitney, West Palm Beach, FL 33410.

[2]Assoc. Prof., School of Civ. and Envir. Engrg., Georgia Inst. of Technol., Atlanta, GA 30332-0355.

[3]Prof., School of Civ. and Envir. Engrg., Georgia Inst. of Technol., Atlanta, GA.

Note. Discussion open until January 1, 1999. To extend the closing date one month, a written request must be filed with the ASCE Manager of Journals. The manuscript for this paper was submitted for review and possible publication on September 15, 1997. This paper is part of the *Journal of Composites for Construction*, Vol. 2, No. 3, August, 1998. ©ASCE, ISSN 1090-0268/98/0003-0126–0131/$8.00 + $.50 per page. Paper No. 16562.

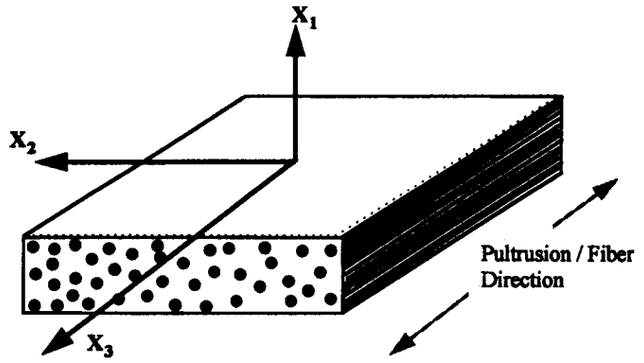


**FIG. 1. Orthogonal Coordinate System and Pultrusion/Fiber Direction**

opment of a technique for the "in-service" monitoring of structural components.

## DESCRIPTION OF MATERIAL

Coupon materials evaluated in this research are cut from plates and angle sections; all are made using a vinylester matrix reinforced with E-glass roving and nonwoven mats. The thicknesses of these coupons range from 6.35 mm (0.25 in.) to 12.7 mm (0.50 in.). The dimensions (length and width) of the specimens used in the ultrasonic immersion tests vary from one test to another and have no bearing on the results of a specific test. To provide a comparison between the different methodologies, many of the specimens are tested using ultrasonic techniques and then using destructive mechanical techniques. When mechanical tests are conducted, the requirements of the mechanical tests dictate the specimen geometry.

Pultruded polymer composites are modeled as transversely isotropic, with the pultrusion direction (fiber direction) perpendicular to the plane of isotropy (as shown in Fig. 1). This assumption allows the stress-strain relations of these materials to be expressed in terms of five independent elastic constants, from which the engineering constants may be calculated (Zureick and Eubanks 1988).

## ULTRASONIC TECHNIQUES IN ANISOTROPIC MATERIALS

For a general anisotropic material, the relationship between ultrasonic phase velocity and the stiffness matrix is given by the Christoffel equation, expressed as

$$(C_{ijkl}l_jl_l - \rho V^2\delta_{ik})\alpha_k = 0 \tag{1}$$

where $V$ = ultrasonic phase velocity that can be measured experimentally; $C_{ijkl}$ = general 9 × 9 stiffness matrix; $\rho$ = material density; $l$ = direction of propagation; $\alpha$ = polarization direction; and $\delta_{ik}$ = Kronecker delta. Since the stiffness matrix is symmetric (due to strain energy considerations), $C_{ijkl}$ is reduced to a 6 × 6 matrix, $C_{mn}$, with 36 components.

To establish the relationship between ultrasonic phase velocities and the material elastic constants, adopt an orthogonal coordinate system ($x_1$, $x_2$, $x_3$) in which the $x_3$ axis coincides with the fiber direction in a unidirectionally reinforced composite (see Fig. 1). For the case of a transversely isotropic material, the 6 × 6 stiffness matrix ($C_{mn}$) is expressed in terms of five independent elastic constants

$$C_{mn} = \begin{bmatrix} C_{11} & C_{12} & C_{13} & 0 & 0 & 0 \\ C_{12} & C_{11} & C_{13} & 0 & 0 & 0 \\ C_{13} & C_{13} & C_{33} & 0 & 0 & 0 \\ 0 & 0 & 0 & C_{44} & 0 & 0 \\ 0 & 0 & 0 & 0 & C_{44} & 0 \\ 0 & 0 & 0 & 0 & 0 & C_{66} \end{bmatrix} \tag{2}$$

where $C_{12} = C_{11} - 2C_{66}$. The engineering constants (such as the longitudinal modulus) can then be calculated from the elastic constants using (Zureick and Eubanks 1988)

$$E_{33} = 4C_{66}\left(1 - \frac{C_{33}C_{66}}{C_{11}C_{33} - C_{13}^2}\right) \tag{3}$$

$$E_{11} = C_{33} - \frac{C_{13}^2}{C_{11} - C_{66}} \tag{4}$$

$$G_{12} = C_{66} \tag{5}$$

$$G_{23} = C_{44} \tag{6}$$

where $E_{33}$ and $E_{11}$ = longitudinal and transverse moduli, respectively; and $G_{12}$ and $G_{23}$ = shear moduli in each plane.

The physics of wave propagation in an anisotropic material is slightly more complicated than those of its isotropic counterpart. For isotropic materials, three types of ultrasonic waves exist as follows: (1) Longitudinal; (2) vertically polarized shear; and (3) horizontally polarized shear. In a longitudinal wave, the particle motion is in the direction of wave propagation, while in the shear waves, the particle motion is perpendicular to the wave propagation direction (note that two possible polarization directions exist, vertical or horizontal, for shear waves in isotropic media). The speeds at which these ultrasonic waves travel are referred to as phase velocities or wave speeds. For the case of an isotropic material, the relationship between the longitudinal wave speed and elastic constants is found from Christoffel's equation [(1)] to be

$$V_L = \sqrt{\frac{\lambda + 2\mu}{\rho}} \tag{7}$$

where $V_L$ = longitudinal wave speed; $\lambda$ and $\mu$ = Lame's elastic constants; and $\rho$ = density of the material.

In an anisotropic material, the directional dependence of the elastic properties of these materials manifests directional dependencies of wave speeds and even particle displacement polarizations. It is useful to introduce the concept of slowness curves to better illustrate these directional properties. The slowness vector, in any given direction, may be defined as the reciprocal of the phase velocity. The slowness diagram (a plot of the slowness vector magnitudes versus direction) of an isotropic material is three concentric spherical sheets. The smallest of the three spherical sheets corresponds to the longitudinal velocity. It is a sphere, since the longitudinal velocity does not change with propagation direction. The other two spherical sheets are identical, since both shear waves travel at the same phase velocity in an isotropic material. For an anisotropic material, the directional dependence of the wave speeds creates a slowness curve that may be nonspherical. Furthermore, two distinct and independent slowness curves for each shear wave may exist. With this in mind, the concept of a quasi-shear wave is needed; a quasi-shear wave is a shear wave that has particle motion that is not purely perpendicular to the wave propagation direction but may have some components of particle displacement in the direction of wave propagation.

Using the coordinate system shown in Fig. 1 and the transversely isotropic assumption, Christoffel's equation [(1)] may be expressed solely in terms of both the five independent elastic constants ($C_{11}$, $C_{33}$, $C_{66}$, $C_{44}$, $C_{13}$) and the phase velocities (wave speeds). Longitudinal waves propagating in the $x_1$ and $x_3$ directions yield the following equations, respectively

$$C_{11} = \rho V_{L11}^2 \tag{8}$$

$$C_{33} = \rho V_{L33}^2 \tag{9}$$

For a shear wave propagating in the 1-2 plane (plane of isotropy), Christoffel's equation [(1)] yields

$$C_{66} = \rho V^2(\theta) \tag{10}$$

For a quasi-shear wave traveling in the 1-3 plane and with polarization of the 1-3 plane, Christoffel's equation [(1)] yields

$$V(\theta) = \sqrt{\frac{b - \sqrt{b^2 - 4c}}{2\rho}} \tag{11}$$

where

$$b = C_{11}\sin^2(\theta) + C_{33}\cos^2(\theta) + C_{44}$$

and

$$c = C_{11}C_{44}\sin^4(\theta) + [C_{44}^2 + C_{11}C_{33} - (C_{13} + C_{44})^2]\sin^2(\theta)\cos^2(\theta) + C_{33}C_{44}\cos^4(\theta)$$

For a transversely isotropic material, the relationships between the surface acoustic wave speed and the elastic constants may be expressed for surface acoustic waves traveling in the principal directions (Royer and Dieulesaint 1984). For a surface acoustic wave traveling in the $x_3$ direction on a free surface that lies in the 1-3 plane, the relationship between elastic constants and phase velocity is given by

$$C_{11}C_{44}\zeta_3^2(C_{33} - \zeta_3) = (C_{44} - \zeta_3)\{C_{11}(C_{33} - \zeta_3) - C_{13}^2\}^2 \tag{12}$$

where $\zeta_3 = \rho V_{R3}^2$ ($V_{R3}$ = phase velocity of the surface acoustic wave traveling in the $x_3$ direction on a free surface that lies in the 1-3 plane). The relationship for a surface acoustic wave traveling in the $x_1$ direction on the same free surface as just mentioned (1-3 plane) is given by

$$C_{11}C_{66}\zeta_1^2(C_{11} - \zeta_1) = (C_{66} - \zeta_1)\{C_{11}(C_{11} - \zeta_1) - (2C_{66} - C_{11})^2\}^2 \tag{13}$$

where $\zeta_1 = \rho V_{R1}^2$ ($V_{R1}$ = phase velocity of the surface acoustic wave traveling in the $x_1$ direction on a free surface that lies in the 1-3 plane). The relationship for a surface acoustic wave that travels in the $x_1$ direction on a free surface that lies in the 1-2 plane is given by

$$C_{33}C_{44}\zeta_2^2(C_{11} - \zeta_2) = (C_{44} - \zeta_2)\{C_{33}(C_{11} - \zeta_2) - C_{13}^2\}^2 \tag{14}$$

where $\zeta_2 = \rho V_{R2}^2$ ($V_{R2}$ = phase velocity of the surface acoustic wave traveling in the $x_1$ direction on a free surface that lies in the 1-2 plane). Note that (12)–(14) are for surface acoustic waves traveling in principal directions. The only surface acoustic waves used in this research travel in one of the previously mentioned principal directions.

## CONTACT TECHNIQUES TO MEASURE $C_{11}$ AND $C_{33}$

The first methodology developed in this work uses a combination of immersion and contact procedures to measure the five independent elastic constants that completely characterize an FRP composite specimen. Eqs. (8) and (9) show that the elastic constants $C_{11}$ and $C_{33}$, respectively, are only dependent upon the longitudinal phase velocities in their corresponding propagation direction. Consequently, $V_{L11}$ and $V_{L33}$ are measured directly using a pair of 1 MHz contact piezoelectric transducers. One transducer is used as the sender and the other is used as the receiver. It is important to note that these contact measurements require a couplant (silicon gel in this case) to couple each transducer to the specimen.

A function generator is used to send two cycles of a sinusoidal signal to the sending transducer; this generates a longitudinal ultrasonic wave that travels through the specimen and is detected on the opposite side by the second (receiving) transducer. The output from the receiving transducer is captured on a 150-MHz digital oscilloscope. The input voltage that is sent from the function generator to the first transducer

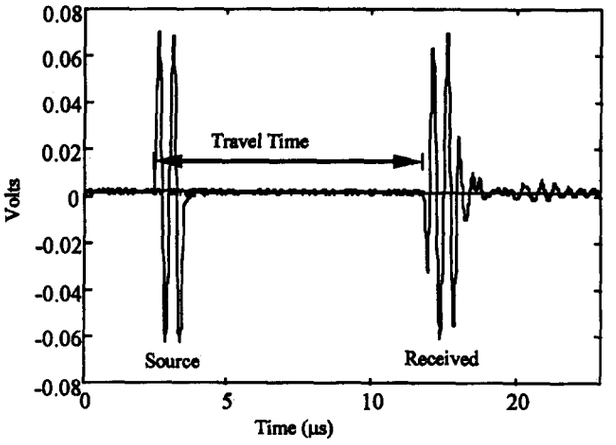


**FIG. 2. Example of Travel Time Measurement**

is also used to trigger the oscilloscope. The delay between the trigger (the time when the ultrasonic wave begins to propagate, or the source) and the arrival of the ultrasonic wave at the receiving transducer is measured (directly on the scope) and used to compute the length of time the longitudinal wave takes to travel through the specimen thickness (see the travel time shown in Fig. 2). This ultrasonic path length is measured using a pair of calipers, so that the corresponding longitudinal phase velocities are calculated by dividing the measured path length by the measured travel time. Note that the specimen densities are measured in accordance with Method A of ASTM D792 with a modification that accounts for the water absorbed by the specimen (Littles 1997). With the specimen densities and longitudinal wave speeds measured, the constants $C_{11}$ and $C_{33}$ are calculated using (8) and (9).

## IMMERSION TECHNIQUES TO MEASURE $C_{44}$, $C_{13}$, AND $C_{66}$

The remaining three independent elastic constants are found using immersion techniques. The immersion setup consists of a tank filled with water and two 3.5-MHz piezoelectric immersion transducers. The specimen is placed in a goniometer directly between the two transducers in the water tank. This allows the angle of the incident ultrasonic wave to be changed by rotating the specimen (see Fig. 3).

Note that the driving frequency of the immersion transducers is 3.5 MHz, while the driving frequency of the contact transducers is 1 MHz. This difference is not due to any experimental requirement but is based on the limitations of existing equipment. A study is developed to investigate any pos-

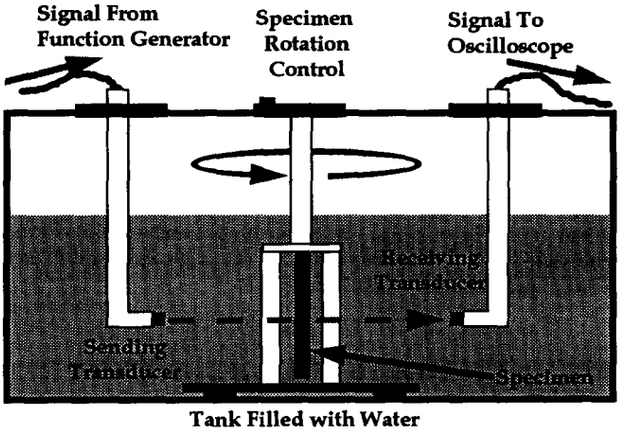


**FIG. 3. Immersion Setup**

sible influence of the driving frequency (1 MHz in the contact tests versus 3.5 MHz in the immersion tests) on the measured longitudinal travel times: a pair of broad-band contact piezoelectric transducers are used to measure longitudinal wave speeds over a wide range of frequencies (between 0.25 and 3.5 MHz). These results (Littles 1997) show that the phase velocities are independent of frequency within the frequency range of this study (0.25–3.5 MHz). As a result, the fact that the immersion and contact transducers are driven with different frequencies has no influence on the measured travel times (and consequently on the elastic constants). It is important to note that this is true since the smallest wavelengths used in this study (on the order of 1.5 mm) are larger than the microstructure of the material; this behavior has been confirmed by previous researchers [for example, Kline and Chen (1988)].

The calculation of the phase velocity in the immersion setup consists of first measuring the time of arrival of a wave that travels through the water path in the absence of the specimen. The arrival of this signal is taken as the initial time, $t_0$. The specimen is then placed in the immersion tank and the arrival times, $t_i$, of the ultrasonic waves are recorded over a range of angles. The velocity of the ultrasonic wave in the specimen is calculated for each incident angle. The equation used for the velocity calculations is given as

$$V(\theta) = \left[\frac{1}{V_w^2} + \frac{\tau^2}{d^2} - \frac{2\tau}{d}\cos(\theta_i)\right]^{-1/2} \tag{15}$$

where $\tau = t_0 - t_i$; $d$ = specimen thickness; $V_w$ = ultrasonic phase velocity in water; $\theta_i$ = angle that the incident wave makes with the specimen, and $\theta$ = angle at which the wave travels in the specimen (Pearson and Murri 1986).

Velocity measurements (as a function of rotation about the $x_2$ axis) are made at 1° increments of an incident angle ($\theta_i$) that varies from 36–62°. This range is chosen because it is beyond the critical angle for these materials; at these angles the only detected wave is the one which has propagated through the specimen as a quasi-shear wave propagating in the 1-3 plane with polarization in the 1-3 plane. This set of measured velocities is used with (11) to calculate the constants $C_{44}$ and $C_{13}$. The Gauss-Newton nonlinear regression method (Chapra and Canale 1988) is used to obtain these constants from the measured set of phase velocities. Note that the $\theta$ used in (11) is equal to $\theta_r$, where $\theta_r$ is determined using Snell's law

$$\frac{\sin(\theta_r)}{V(\theta)} = \frac{\sin(\theta_i)}{V_w} \tag{16}$$

To measure the shear wave speed as a function of angle of rotation about the $x_3$ axis, the previously described procedure is repeated for angles about the $x_3$ axis. The velocity data for this specimen orientation is used with (10) to calculate $C_{66}$. Note that $C_{66}$ (and hence the shear wave speed propagating in the 1-2 plane and polarized in the 1-2 plane) is not a function of rotation angle about the $x_3$ axis. Consequently, the same values should be measured no matter what incident angle is used. However, these measurements are made over the same range as in the previous case to account for any experimental error that may occur and (most importantly) are used as a check on the transversely isotropic assumption. The average value of these 26 measurements is taken to be the actual $C_{66}$ value. It is critical to note that the standard deviations of the $C_{66}$ values are quite small [generally below 1% of the average value (Littles 1997)], thus confirming that the assumed transversely isotropic characterization of the pultruded material is correct.

## CONTACT AND IMMERSION EXPERIMENTAL RESULTS

The combined immersion and contact procedures are used to examine samples cut from angle and plate members with nominal specimen thicknesses of 6.35 mm (¼ in.), 9.53 mm (⅜ in.), and 12.7 mm (½ in.) (Littles 1997). As an example, the engineering constants are found (nondestructively) for a 152.4 mm by 152.4 mm (6 in. by 6 in.) polyester-reinforced angle section with nominal thicknesses of 9.53 mm (⅜ in.). This particular experiment is chosen because the member geometry enables mechanical tests to be conducted to determine $E_{11}$ as well as $E_{33}$. Due to specimen grip requirements, the specimen length required to conduct uniaxial compression tests for this thickness is approximately 139.7 mm (5.5 in.). Consequently, specimens are cut out of a pultruded 152.4 mm by 152.4 mm (6 in. by 6 in.) angle member with their length in either the $x_3$ or $x_1$ direction. This enables a comparison to be made between the mechanical (destructive) and combined ultrasonic contact and immersion (nondestructive) techniques for values of $E_{11}$ and $E_{33}$. The specimens are loaded in compression at a constant rate of 1.27 mm/min (0.05 in./min) and a length of 63.5 mm (2.5 in.) is placed in the grips at either end.

A comparison of the results from the nondestructive (ultrasonic contact and immersion) and destructive mechanical (uniaxial compression using ASTM D3410) tests are given in Tables 1 and 2. Note that these tables only present one of the moduli for each of the destructive mechanical tests ($E_{33}$ in Table 1 and $E_{11}$ in Table 2). This demonstrates a limitation of the mechanical tests; destructive techniques yield only one of the engineering constants for each specific test, whereas the nondestructive techniques yield all five independent elastic constants for each specimen tested (from which all of the engineering constants are calculated). Note that the mechanical results of shear moduli are not presented in Tables 1 or 2, because none of these are mechanically tested in shear. It should also be noted that the shear moduli values obtained in the nondestructive tests are higher than expected, especially $G_{23}$. This demonstrates one of the problems with the proposed nondestructive tests; it is difficult to obtain accurate shear moduli with the combined ultrasonic contact and immersion technique. However, current research is developing an accurate single-sided technique.

An investigation is conducted to observe the spatial variation of engineering constants for a 152.4 mm by 152.4 mm (6 in. by 6 in.) angle specimen. The nondestructive procedure is

**TABLE 1. Comparison of Nondestructive with Destructive (ASTM D3410) Test Results for $E_{33}$**

| | Nondestructive measurements | | | | Destructive measurements | |
|---|---|---|---|---|---|---|
| Specimen (1) | $E_{33}$ (GPa) (2) | $E_{11}$ (GPa) (3) | $G_{23}$ (GPa) (4) | $G_{12}$ (GPa) (5) | $E_{33}$ (GPa) (6) | Difference (%) (7) |
| 1 | 24.86 | 8.39 | 6.83 | 4.28 | 25.99 | −4.3 |
| 2 | 23.90 | 8.39 | 6.97 | 4.23 | 22.83 | +4.7 |
| 3 | 23.39 | 7.03 | 6.12 | 4.24 | 21.68 | +7.9 |
| 4 | 23.72 | 7.35 | 6.24 | 4.23 | 22.27 | +6.5 |

**TABLE 2. Comparison of Nondestructive with Destructive (ASTM D3410) Test Results for $E_{11}$**

| | Nondestructive measurements | | | | Destructive measurements | |
|---|---|---|---|---|---|---|
| Specimen (1) | $E_{33}$ (GPa) (2) | $E_{11}$ (GPa) (3) | $G_{23}$ (GPa) (4) | $G_{12}$ (GPa) (5) | $E_{11}$ (GPa) (6) | Difference (%) (7) |
| 5 | 24.54 | 8.20 | 6.61 | 4.24 | 8.67 | −5.4 |
| 6 | 24.77 | 8.17 | 6.68 | 4.26 | 8.43 | −3.1 |
| 7 | 24.39 | 7.26 | 6.32 | 4.15 | 8.85 | −18.0 |

performed at ten locations along the $x_1$ axis, each separated by 10 mm, to observe changes in local properties perpendicular to the pultrusion direction. The nondestructive procedure is again performed at 10 locations along the $x_3$ axis, each separated by 10 mm, to observe changes in local engineering constants along the pultrusion direction. As expected, the constants changed more along the $x_1$ direction than along the $x_3$ direction (pultrusion direction). For example, $E_{11}$ changed by $\pm 6.0\%$ of its average along the $x_1$ direction but only by $\pm 2.85\%$ of its average along the $x_3$ direction. Likewise, $E_{33}$ changed by $\pm 5.5\%$ of its average along the $x_1$ direction but only by $\pm 2.7\%$ of its average along the $x_3$ direction. The local variation in engineering constants found in this experiment, due to the spatial variation of the material, shows that exact agreement between the destructive and nondestructive techniques is not to be expected.

## SURFACE ACOUSTIC WAVE PROCEDURE

For this procedure, the first two elastic constants ($C_{11}$ and $C_{33}$) are found using the contact techniques (previously described), while the remaining three elastic constants are found using surface acoustic waves. These surface acoustic waves are generated and detected using optical techniques (Bruttomesso et al. 1997). The optical detection system requires a reflective surface, but the original finish on both the polyester and vinylester reinforced specimens has sufficient reflectivity and no additional preparation is required. However, the measurement of waves on any cut surface (e.g., on the plane perpendicular to the pultrusion direction) did require surface preparation; these surfaces are sanded to increase their reflectivity to an acceptable level.

The surface acoustic waves are generated using a 9-mJ Q-switched, 15-ns pulse length, Nd:YAG laser, which produces a 1,064-nm wavelength beam. A heterodyne interferometer is used to detect the arrival of the surface acoustic waves. This interferometric detector uses a 2-W continuous argon ion laser that produces a beam with a wavelength of 514.5 nm. A complete description of this detection system, which measures absolute particle velocities of a point on the surface, is given by Bruttomesso et al. (1993).

The phase velocities of the surface acoustic waves are obtained by measuring the travel times of these waves across known distances. This is accomplished by generating the surface acoustic wave with the Nd:YAG source and then measuring the surface acoustic wave with the interferometric detector. The generation source is moved a known distance closer

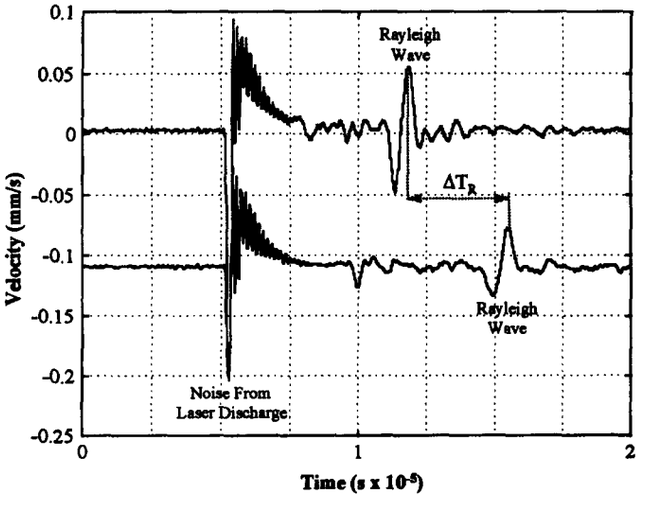


**FIG. 4. Example of Measurement of Surface Acoustic Wave Travel Time**

**TABLE 3. Comparison of Surface Acoustic Wave and Immersion Test Results**

| Technique (1) | Engineering Constants $E_{33}$ (2) | $E_{11}$ (3) | $G_{23}$ (4) | $G_{12}$ (5) |
|---|---|---|---|---|
| Surface acoustic wave technique (GPa) | 25.71 | 8.85 | 3.66 | 7.10 |
| Immersion technique (GPa) | 24.32 | 8.94 | 4.51 | 4.99 |
| Difference (%) | −5.4 | +1.0 | +23.4 | −29.7 |

to the detector (using a micrometer on the translation stage), and another surface acoustic wave is then generated and measured at this new distance. The surface wave velocity is calculated by dividing the difference in arrival times of the two surface acoustic waves ($\Delta T_R$) by the distance between the two generation points, as shown in Fig. 4. Ten individual waves are averaged at each location to increase the signal-to-noise ratio.

The surface acoustic wave velocities are calculated for waves traveling along the $x_3$ direction on the free surface lying in the 1-3 plane, waves traveling in the $x_1$ direction on the same free surface, and waves traveling in the $x_1$ direction on the free surface lying in the 1-2 plane. With $C_{11}$ and $C_{33}$ known, the constants $C_{13}$ and $C_{44}$ are found by solving (12) and (14) simultaneously using the corresponding experimentally measured wave speeds. $C_{66}$ is found by solving (13) for $C_{66}$, using the corresponding experimentally measured wave speeds.

## SURFACE ACOUSTIC WAVE EXPERIMENTAL RESULTS

The surface acoustic wave technique is used to calculate the engineering constants for specimens cut from angle and plate members with nominal specimen thicknesses of 6.35 mm (¼ in.), 9.53 mm (⅜ in.), and 12.7 mm (½ in.) (Littles 1997). An example of typical results for the surface acoustic wave technique is given for coupons cut from a 101.6 mm by 101.6 mm (4 in. by 4 in.) vinylester-reinforced angle member with a nominal thickness of 6.35 mm (0.25 in.). The immersion technique is also used to calculate the engineering constants on the exact same specimen. A comparison of the Young's and shear moduli is seen in Table 3.

This comparison shows that the values of $E_{33}$ and $E_{11}$ are quite close from one method to the other, whereas the shear values are somewhat less consistent. However, the measurements for $G_{12}$ are not made in the same location for each technique, which may have a significant effect on the test results, since the engineering constants have been shown to vary significantly over a given specimen. It should be noted that destructive in-plane shear tests have been conducted on V-notched beam specimens of similar size and material (Zureick and Scott 1997); these results report an in-plane shear modulus of 4.2 GPa, with a coefficient of variation of 8%.

## CONCLUSIONS

The application of FRP composites for structural highway applications has created the necessity to completely characterize the engineering constants of these materials. A combination of immersion and contact ultrasonic methodologies with surface acoustic wave measurements are used to investigate the feasibility of applying ultrasonic wave speeds to characterize this material. The surface acoustic wave technique has the benefit that it does not require the specimen to be placed in an immersion tank, thus allowing specimens of any size or geometry to be interrogated. A comparison of the experimental results shows that ultrasonic techniques yield modulus values

that are quite close to those obtained using mechanical tests. However, these nondestructive methodologies have several advantages including that all of the engineering constants are measured for a single specimen, that the measurements are made over a local volume of material, so that it is possible to evaluate spatial variations within a specimen, and the potential for in-service monitoring of components or tracking time-dependent material properties in long-term tests exists.

## ACKNOWLEDGMENTS

This work is supported by the Federal Highway Administration under contract No. DTFH61-93-C-0012. Eric Munley serves as program director.

## APPENDIX. REFERENCES

Bruttomesso, D. A., Jacobs, L. J., and Costley, R. D. (1993). "Development of an interferometer for acoustic emission testing." *J. Engrg. Mech.*, ASCE, 119(11), 2303–2316.

Bruttomesso, D. A., Jacobs, L. J., and Fiedler, C. (1997). "Experimental and numerical investigation of the interaction of Rayleigh surface waves with corners." *J. Nondestructive Evaluation*, 16(1), 21–30.

Chapra, S. C., and Canale, R. P. (1988). *Numerical methods for engineers*, McGraw-Hill Inc., New York, N.Y.

Kim, K. Y., Ohtani, T., Baker, A. R., and Sachse, W. (1995). "Determination of all elastic constants of orthotropic plate specimens from group velocity data." *Res. in Nondestructive Evaluation*, 7(1), 13–29.

Kline, R. A., and Chen, Z. T. (1988). "Ultrasonic technique for global anisotropic property measurement in composite materials." *Mat. Evaluation*, 46, 986–992.

Littles, J. W. Jr. (1997). *Ultrasonic characterization of fiber reinforced polymeric (FRP) composites*, PhD dissertation, Georgia Inst. of Technol., Atlanta, Ga.

Park, H., and Calder, C. (1994). "Laser generated Rayleigh waves in graphite/epoxy composites." *Experimental Mech.*, 34(2), 148–154.

Pearson, L. H., and Murri, M. J. (1986). "Measurement of ultrasonic wave speeds in off-axis directions of composite materials." *Review of progress in QNDE*, Thompson and Chimenti, eds., Vol. 5, 1093–1101.

Rose, J. L., Nayfeh, A., and Pilarski, A. (1990). "Surface for material characterization." *J. Appl. Mech.*, 57, 7–11.

Royer, D., and Dieulesaint, E. (1984). "Rayleigh wave velocity and displacement in orthorhombic, tetragonal, hexagonal, and cubic crystals." *J. Acoustical Soc. Am.*, 6(5), 1438–1444.

Stijnman, P. W. A. (1995). "Determination of elastic constants of some composites by ultrasonic velocity measurements." *Composites*, 26(8), 597–602.

Zimmer, J. E., and Cost, J. R. (1970). "Determination of the elastic constants of a unidirectional fiber composite using ultrasonic velocity measurements." *J. Acoustical Soc. Am.*, 47(3), Pt. 2, 795–803.

Zureick, A. H., and Eubanks, R. A. (1988). "Spheroidal cavity with prescribed asymmetric tractions in three-dimensional transverse isotrophy." *J. Engrg. Mech.*, ASCE, 114(1), 24–48.

Zureick, A. H., and Scott, D. (1997). "Short term behavior and design of fiber-reinforced polymeric slender members under axial compression." *J. Composites Constr.*, 1(4), 140–149.